An assessement of global energy resource economic potentials, supplementary material

S.1. Introduction and use of the supplementary material

This part of the work aims to complement the main paper by providing all details that would be required by anyone who might be interested in either:

- Verifying the methodology or reproduce the results
- Rebuilding this database for use in conjunction with a particular model of energy systems

A high amount of care was put into summarising compactly all relevant information in this part of the work in order to make this possible. Mathematical details underlying the calculations given in the main text are provided. Additionally, lists of data are given for a chosen set of world regions, which may not necessarily correspond to the particular divisions of other research groups. It is however impractical to provide larger tables involving all countries of the world, even though such tables exist underlying this work. For more information, the authors may be contacted at the address provided.

S.2. Distribution functions and cost-supply curves

S.2.1. Distribution function for the hierarchical type of resources

Hierarchical resources have an exponential energy distribution in productivity space:

$$f(\nu)d\nu = \begin{cases} \frac{A}{\sigma} e^{-\frac{\nu}{\sigma}} d\nu & \nu > \mu \\ 0 & \nu \leq \mu \end{cases} . \tag{1}$$

This function is required in cost space, and the equation connecting cost to productivity is

$$C = \frac{C_{var}}{\nu} + C_0. \tag{2}$$

where C_{var} corresponds to costs per unit productivity such as the rent of the land (in \$/km^2), while C_0 is the sum of fixed costs (in \$/GJ). The density productivity interval must be transformed into a cost interval:

$$dC = -\frac{C_{var}}{\nu^2} d\nu, \quad \Rightarrow d\nu = -\frac{C_{var}}{(C - C_0)^2} dC. \tag{3}$$

Using a cost scaling parameter $B = C_{var}/\sigma$, the distribution becomes:

$$f(C)dC = \begin{cases} \frac{AB}{(C-C_0)^2} e^{-\frac{B}{C-C_0}} dC & C > C_{fixed} \\ 0 & C \leq C_0 \end{cases} . \tag{4}$$

S.2.2. Distribution function for nearly identical resources

In the case of nearly identical resources, there is no exact convenient analytical form that can be derived from eq. 2 of the paper. However, the form given in eq. 4 works very well, and can be derived from eq. 2 through a simple approximation.

Nearly identical energy producing resources, such as land plots, are assumed truly identical, and therefore have a potential situated at a single value of productivity $\nu = \mu$,

$$n(\nu)d\nu = N\delta(\nu - \mu)d\nu, \tag{5}$$

where n is a density of energy producing land area, while N is the total energy producing land area (in km^2) and the function $\delta(\nu)$ is the Dirac delta function[1]. Without any additional reductions in productivity, the total amount of energy that can be obtained from these land resources would be their area times the productivity:

$$A = \int_0^\infty \nu N\delta(\nu - \mu)d\nu = N\mu. \tag{6}$$

Unit land areas have a suitability factor, however, that reduces their productivity below the maximum value of μ by a small amount ϵ with a probability P. The probability for the reduction in productivity is assumed to be normally distributed around zero, with standard deviation σ, but positive:

$$P(\epsilon)d\epsilon = \begin{cases} \frac{1}{\sqrt{2\pi}\sigma} e^{-\frac{\epsilon^2}{2\sigma^2}} d\epsilon & \epsilon \leq \mu \\ 0 & \epsilon > \mu \end{cases}, \tag{7}$$

where the reduction in productivity ϵ must be less than the maximum value μ. The distribution of resources must be calculated by summing over all reduction values ϵ given their probability $P(\epsilon)$:

$$n'(\nu)d\nu = \int n(\nu)P(\epsilon)d\epsilon = \int_0^\mu \frac{N}{\sqrt{2\pi}\sigma} e^{-\frac{\epsilon^2}{2\sigma^2}} \delta(\nu - \epsilon - \mu)d\nu d\epsilon. \tag{8}$$

This can be seen as a sum of several Dirac Delta functions centred at slightly reduced values of productivity, $\mu - \epsilon$, with probability $P(\epsilon)$, instead of one Dirac Delta function centred at μ with probability 1. The total amount of energy that can be obtained from each plot of land corresponds to its area times its productivity. Thus, the productivity distribution of energy production potential leads to eq. 2 of the main paper:

$$g(\nu)d\nu = \nu n'(\nu)d\nu = \begin{cases} \frac{N}{\sqrt{2\pi}\sigma} \nu e^{-\frac{(\nu-\mu)^2}{2\sigma^2}} d\nu & \nu \leq \mu \\ 0 & \nu > \mu \end{cases}. \tag{9}$$

This function is required in cost space, and the equation connecting cost to productivity is

$$C = \frac{C_{var}}{\nu} + C_{fixed}, \tag{10}$$

where C_{var} corresponds to, for instance, the rent of the land (in \$/km^2), while C_{fixed} is the sum of fixed costs (in \$/GJ). The productivity is situated very near the value of μ, since the variations of productivity are small and $\sigma << \mu$. ν can be rewritten as a small variation around μ, i.e. $\mu - \Delta$:

$$C = \frac{C_{var}}{\mu - \Delta} + C_{fixed} = \frac{C_{var}/\mu}{1 + \Delta/\mu} + C_{fixed} \simeq \frac{C_{var}}{\mu}\left(1 - \frac{\Delta}{\mu}\right) + C_{fixed} = \frac{C_{var}}{\mu}\left(1 + \frac{\nu - \mu}{\mu}\right) + C_{fixed}, \tag{11}$$

which is the crucial approximation, and

$$\nu = (C - C_{fixed})\frac{\mu^2}{C_{var}} = (C - C_0)\frac{\mu^2}{C_{var}} + \mu, \tag{12}$$

[1]The Dirac delta function is defined such that $\int_{-\infty}^{\infty} \delta(x - a)f(x)dx = f(a)$ is true.

where C_0 is defined as the sum of fixed costs plus C_{var}/μ, the total cost at the maximum productivity value. Since $dC = -C_{var}/\mu d\nu$, the density can be rewritten as

$$g(C)dC = \begin{cases} \frac{N}{\sqrt{2\pi}B}\left((C-C_0)\frac{\mu^2}{C_{var}}+\mu\right)e^{-\frac{(C-C_0)^2}{2B^2}}dC & C > C_0 \\ 0 & C \leq C_0 \end{cases}, \tag{13}$$

where the new parameter B is defined as $C_{var}\sigma/\mu^2$. This can be rewritten further as

$$g(C)dC = \begin{cases} \frac{N}{\sqrt{2\pi}B}\mu\left(\frac{C-C_0}{B}\frac{\sigma}{\mu}+1\right)e^{-\frac{(C-C_0)^2}{2B^2}}dC & C > C_0 \\ 0 & C \leq C_0 \end{cases}. \tag{14}$$

The value of C cannot be below C_0 by definition, but also, $f(C)dC$ decreases rapidly to zero as $C - C_0$ becomes larger than B. Therefore, the value of the term $(C - C_0)/B$ is mostly less than one wherever a significant potential of energy exists. Since σ is much smaller than μ, this results with

$$\frac{\sigma}{\mu}\frac{C-C_0}{B} << 1, \tag{15}$$

and therefore the distribution becomes

$$g(C)dC = \begin{cases} \frac{A}{\sqrt{2\pi}B}e^{-\frac{(C-C_0)^2}{2B^2}}dC & C > C_0 \\ 0 & C \leq C_0 \end{cases}, \tag{16}$$

where now $A = N\mu$ is the total energy potential.

This is the strict region of validity of the expression given in 4 of the paper. In numerical terms, it is empirically found that the rigidity of these rules can be relaxed and the validity extended. For example, the distribution in productivity space can actually have a tail towards higher values or have a large value for σ, and this does not significantly alter the goodness of fit of the function in cost space.

S.2.3. Cost-supply curve expressions

From the distributions $f(C)dC$, cumulative distributions $N(c)$ can be derived. For hierarchical resources, this results in

$$N(C) = A\,e^{\left(-\frac{B}{C-C_0}\right)}, \tag{17}$$

while for nearly identical resources this is

$$N(C) = A\,\mathrm{erf}\left(\frac{(C-C_0)}{\sqrt{2}B}\right), \tag{18}$$

where 'erf' is the error function.

The cost-supply curves are the inverse of these functions, which respectively give

$$C(N) = \frac{-B}{\ln\left(\frac{N}{A}\right)} + C_0 \tag{19}$$

and

$$C(N) = \sqrt{2}B\,\mathrm{inverf}\left(\frac{N}{A}\right) + C_0, \tag{20}$$

where 'inverf' is the inverse error function.

S.2.4. Parameterisation formulas

In order to define a particular distribution or cost-supply curve, the parameters A, B and C_0 are required, while the data available usually involves the total technical potential of the resource and a fraction of this considered to exist at costs situated between two values, as well as the current level of use of the resource. Assuming that two points of the curve are known, this may be expressed as two quantities Q_1 and Q_2 which occur at two cost values C_1 and C_2. These quantities can be expressed as fractions of the total technical potential, δ_1 and δ_2, the latter corresponding to the parameter A. In the case of the distribution for hierarchical resources, the values of B and C_0 are the following:

$$C_0 = \frac{C_2 \ln \delta_2 - C_1 \ln \delta_1}{\ln \delta_2 - \ln \delta_1}, \tag{21}$$

$$B = -(C_1 - C_0) \log \delta_1. \tag{22}$$

In the case of nearly identical resources, this becomes

$$B = \frac{C_2 - C_1}{\sqrt{2}(\mathrm{inverf}\,\delta_1 - \mathrm{inverf}\,\delta_2)}, \tag{23}$$

$$C_0 = \sqrt{2} B\, \mathrm{inverf}\,\delta_1 + C_1 \tag{24}$$

S.2.5. Demonstrating the validity of the functional forms using IMAGE data

Examples of the use of the analytical forms of the distributions are presented in figure S.4.1 for biomass, solar and wind energy. The data are taken from land use simulations performed using IMAGE by Hoogwijk et al. (2009, 2004); Hoogwijk (2004), which provide the only sources of cost-supply curves calculated outside of this project that do not already use assumptions on the analytical form of the resource distribution. Since IMAGE simulates the use of the land on each point of a global grid, and since these cost-supply curves were calculated by building histograms of the number of grid points with productivities situated within various ranges, their form stems purely from the statistical nature of the data. These are thus appropriate for testing the functions given above.

Non-linear least-squares fits were performed with both analytical forms for each data set. In every case, only one of the two functions given above is appropriate, while the other is not. Fits are moreover of exceptional quality. For instance, wind resources are the best example of resources of the hierarchically ordered type, which stems from the exponentially increasing number of simultaneous factors required to produce ever higher productivities. The data is found to follow almost exactly the distribution for hierarchical resources (note that the deviation at low cost values stems from the aggregation of a region with a different cost structure into the region for Canada). Meanwhile, solar resources represent the best example of nearly identical resources, since in regions of similar irradiation, all sun-facing areas are equivalent. The data is found to follow closely the distribution for nearly identical resources. Biomass resources from abandoned agricultural land are nearly identical. This stems from the similar nature of local areas of agricultural land (i.e. large plains, deltas, similar irradiation, etc). Land plots with lower productivity are used for other activities. Rest land, however, is the category of land which would not be used for agriculture, and can be of various nature, but includes mainly savannah, shrubland and grassland or steppe. These can be ordered, and can be seen to follow the distribution for hierarchical resources.

S.3. Cost-supply curve calculation methodology per resource type

S.3.1. Definition of world regions

Cost-supply curves were calculated in this work for every E3MG world regions from aggregations of data defined for 179 countries. However, the region definition in E3MG is very specific and does not correspond closely to that of most other global models, and tables provided here for E3MG regions would be of limited use to the global modelling community. For accuracy, data for 179 countries would be required to be provided here, but is not possible for space considerations. For the convenience of potential users, the results are provided in tables with a definition of regions resembling that of other models such as IMAGE, AIM, etc. Any other aggregation of data, in table or curve form, can be supplied by the authors upon request. Table S.4.1 gives the list of regions used here with most countries that belong to them.

S.3.2. Wind and solar energy

Following the justification of section S.2.5, wind resources were modelled using a distribution of hierarchical type, while solar resources were modelled using a distribution for nearly identical resources. In both cases simulations performed by Hoogwijk et al. (2004) (wind energy) and Hoogwijk (2004) (PhD thesis, wind, solar and biomass energy) using IMAGE 2.2 were used, published in the form of data tables featuring both technical potentials and interpolations through cost supply curves at specific cost values for a list of 17 world regions. These values were used to find the distribution parameters A, B and C_0 for every one of their regions. A values were thus obtained without additional processing, while B and C_0 values were obtained using equations 21 to 24.

However, the regional aggregation the work of Hoogwijk *et al*. does not match exactly the one chosen for this work (or the one used in E3MG), detailed in section S.3.1. In order to obtain curves for this set of world regions, energy potentials from IMAGE 2.2 regions were disaggregated into 179 countries, and subsequently re-aggregated. This required additional assumptions in particular cases where A values were required to be divided between underlying countries[2]. In the case of wind energy, the division of A values was done proportionally to the cube of the yearly averated wind speed[3] (obtained from UNEP, 2011; 3TIER, 2011b), times the amount of land suitable in each country for these energy production activities (the land area (CIA, 2011) times the suitability factor provided by Hoogwijk *et al*., assumed the same for all countries member of a region). In the case of solar energy, A values were divided proportionally to the insolation averaged over countries (obtained from 3TIER, 2011a; UNEP, 2011) times the amount of land suitable in each country. Assuming an identical shape for the cost supply curves (identical values of B and C_0) for every country within a particular IMAGE region, and using A values thus divided, cost supply curves for the 179 countries were built. Given this set of curves, the re-aggregation of curves into new world regions was performed by summing the energy potential values at each cost (i.e. a sum along the horizontal axis of the cost-supply curve, called a horizontal sum henceforth). These aggregated curves do not correspond anymore to pure distributions of either type, but do not differ significantly from pure forms in any of the regions chosen for this work. Thus, new values for A, B and C_0 for this work's regional definition were re-estimated using equations 21 to 24, for the sake of simple presentation in this work (avoiding listing parameters for 179 countries, or providing aggregate curves defined on large numbers of cost data points). For E3MG, data curves evaluated on 1000 cost data points are used directly instead.[4]

Cost values with which cost-supply curves were calculated using equations 21 to 24 were also obtained from Hoogwijk et al. (2004); Hoogwijk (2004), but were rescaled to 2008 prices. This procedure, however, generates costs of energy production slightly different (wind) or higher (solar) than recent estimates available from IEA (2010b), due to small errors (wind) or significant learning-by-doing cost reductions (solar) stemming from economies of scale with large expansion of electricity generation capacities that occurred between 2004 and 2008. The curves were therefore recalibrated with a constant offset to match recent values from IEA (2010b). The results are provided in table S.4.3 for this work's list of world regions.

S.3.3. Hydropower

Hydroelectric resources, highly site dependent, were modelled using the distribution for hierarchical resources. Hydroelectric potentials and current annual electricity generation values were obtained from IJHD (2011), while the costs were obtained using an extensive study of 250 recent projects by Lako et al. (2003) from which statistics were derived. These statistics were performed for the countries studied in Lako *et al*., and were used as proxies for regions not studied in their work, or where no information on recent hydroelectric developments was found. Some countries do not have recently reported hydroelectric projects onto which to base cost values.

Recent developments have hardly followed an order of cost, since they were scattered between 500 and 4000 2003USD/kW. In order to use a cost-supply curve, it can only be assumed that future developments actually will approximately follow a cost order. Although only approximately true, this is reasonable, since development costs *will* significantly increase when more and more usable sites are depleted, irrespective of the particular order in which

[2]Note that this is mostly true for E3MG regions; the regions used for this paper are very similar to those used by Hoogwijk *et al*.

[3]Wind energy scales with the cube of the average wind speed averaged over time (see for instance Sørensen (2011)).

[4]Exact analytical forms for cost-supply curves correspond to the inverse the cumulative distribution. When the cumulative distribution involves the sum of several distributions, an analytical form for the cost-supply curve does not exist.

they were built, and only difficult or distant river basins remain. This is important since the costs of hydroelectricity are currently not high in comparison to alternatives, but the resources are limited, and therefore the development of hydroelectric resources must be limited through an increasing cost in models of power systems such as FTT:Power.

As can be seen in the current hydroelectricity generation data compared to the data for hydroelectric potentials in IJHD (2011) (or alternatively WEC (2010)), a significant portion of the technical potential of every region is already developed. The cost values delimiting the technical and economic potentials amongst remaining potential hydroelectric sites are not given by IJHD (2011). Since the distribution of costs is not symmetrical, the assumption was taken that the amount of resources considered economical lies at costs between the local average cost μ minus its standard deviation δ, $\mu - \delta$, and plus twice its standard deviation $\mu + 2\delta$. This puts the upper cost limit to around 5000 2008USD/kW. Thus, sites within the technical potential with costs higher than this are considered currently uneconomical. Given this definition, a cost-supply curve for each region was calculated. Parameters for each regional cost-supply curve are given in table S.4.3. The global cost-supply curve of figure 3 of the main text is an aggregation (a horizontal sum) of these regional curves.

S.3.4. Geothermal energy

Geothermal resources were divided into two groups, occurring in either "in belt" or "out of belt" land areas, referring to the so-called volcanic belt. "In belt" areas are located in volcanically active zones with high geothermal gradients (temperature gradients with bore depth from the surface of the ground). Given the particular characteristics of geothermal active areas in terms of their heat storage and underground temperature variation, the extraction of geothermal resources in those places are highly site-specific, and were therefore modelled using a hierarchical distribution. "Out of belt" areas corresponds to the rest of the continental masses, with sites that are characterised by smaller geothermal gradients, and that are almost identical to one another within large geographical areas. "Out of belt" resources were thus modelled using a distribution for nearly identical resources. The ratio of "in belt" to "out of belt" land area values were obtained from EPRI (1978), enabling to divide reported technical potentials into two A values for each distribution type. Geothermal resources were moreover calculated for both hydrothermal and EGS dry rock technologies, yielding four sets of parameters. Each cost-supply curve in each region was obtained by aggregating four curves.

Technical potentials for different world regions were obtained from Bertani (2012). Given the differences between their regional aggregation and this work, the same methodology was used as for wind and solar energy in order to disaggregate the regional technical potentials between the same 179 countries. The proportion of the regional technical potentials assigned to every country within a particular region was assumed to be proportional to the total amount of geothermal energy stored up to five kilometres of depth in each country, obtained from Aldrich et al. (1981).

Cost values for geothermal electricity production were taken from IEA (2010c). It was assumed that 90% of the resources 'in belt' were situated within these ranges of costs. However, resources 'out of belt' follow the distribution for nearly identical resources, but face higher costs due to lower geothermal gradients and less productivity per unit investment. Since no additional cost information was available in this regard, these resources were assumed to lie in the upper half of the cost range given by IEA (2010c).[5] Table S.4.5 gives the parameters that can be used to reproduce these cost-supply curves using both types of distributions.

The lower boundary curve of the uncertainty range assumes a technical potential of 4 EJ/y based on differing assumptions for both technologies. In the case of hydrothermal technology, a conservative potential estimate of 70 GW (2 EJ/y) was derived by limiting the calculation to well known sites that have been already characterised by direct involvement or informed calculations (Bertani, 2010, 2012). Meanwhile, the limited amount of accumulated experience with EGS technology creates uncertainties in the evaluation of the technical potential through variations in the efficiency of extraction (Tester and Anderson, 2006), leading Bertani to estimate a lower limit of 70 GW (2 EJ/y). The upper boundary of the uncertainty range involves yet another set of assumptions for both hydrothermal and EGS technologies. In the case of hydrothermal, according to estimations made by (Stefansson, 2005), undiscovered or additional resources could exist which would be five to ten times higher than identified resources, increasing the

[5] In 'out of belt' areas, the same technologies are involved, either for hydrothermal or EGS, as for 'in belt' areas. However, the resources are nearly identical over large areas and of equally low quality in comparison to 'in belt' areas. Significantly higher productivities are found in volcanic areas.

potential to 1000-2000 GW (57 EJ/y). In the case of EGS, the technical potential is calculated by an extrapolation of resources in the United States to the global level using the proportion between the heat stored at depths of less than 10 km in the United Stated with the known EGS primary energy potential in the same region, estimated by Tester and Anderson (2006) as 1×10^6 EJ of heat stored per 2.61 EJ/yr of EGS primary energy potential. Using the estimation of the heat stored at depths less than 10 km on the global scale produced by Rowley (1982) of 403×10^6 EJ, this estimation results in a global technical potential of 54 EJ/yr, yielding a total of 111 EJ/y.

S.3.5. Bioenergy

Four bioenergy cost-supply curves are given in figure 3 of the main text, for each of the SRES scenarios A1, A2, B1 and B2, based on simulations performed using IMAGE 2.2, available in Hoogwijk et al. (2005, 2009); Hoogwijk (2004) (see IPCC (2000) for information on SRES scenarios). The primary biomass energy sources considered in the cost supply curve are abandoned agricultural land, low-productivity land, rest land and bagasse, where the first is the largest source in all scenarios. Following the justification of section S.2.5, abandoned agricultural land was modelled using distributions for nearly identical resources, while rest land was modelled using distributions for hierarchical resources. The other two types of primary biomass resources, bagasse (from WEC (2010)) and low-productivity land (from Hoogwijk et al. (2005)) contribute very small fractions of the total potentials, and their technical potentials were simply added to the potentials of abandoned agricultural land and rest land respectively, for every region in every scenario. Cost values, however, are only given by Hoogwijk *et al*. for the total amount of biomass resources in each region, not individually for abandoned agricultural and rest land. Therefore, the right distribution to use had to be determined, by deciding which of the two represented best the data. This corresponds to finding the *dominant* distribution. Therefore, the appropriate *type* of distribution was determined by visual inspection for each region. Potentials for abandoned agricultural land are for most regions much larger than those for rest land, and therefore most regions were modelled using distributions for nearly identical resources. These distributions were disaggregated into 179 countries, following the methodology described in section S.3.2, proportionally to country land areas times their suitability factor. Table S.4.4 provides values that can be used to parameterise biomass cost-supply curves for the world regions used in this work, with the appropriate type of distribution used indicated in the last column.

S.3.6. Ocean energy

Given the vast extent of oceans, the calculation of theoretical potentials for ocean energy sources produces large values. For instance, using a global wind-wave model, Mork et al. (2010) estimated a potential for wave energy between 2986 and 3703 GWe (94 to 117 EJ/yr) , while Charlier and Justus (1993) estimated a global theoretical tidal power potential between 1000 and 3000 GWe (32 to 95 EJ/yr) using a capacity factor of 100%. In the case of ocean thermal energy, Pelc and Fujita (2002) estimated a theoretical potential of approximately 10 TW (315 EJ/yr) using a capacity factor of 100%, while for salinity gradient energy, Cavanagh et al. (1993) calculated a value of 2.6 TW (82 EJ/yr) using a capacity factor of 100%. Using values from these particular studies, the total theoretical potential for ocean energy would be as high 523 and 619 EJ/yr. However, more reliable and conservative potentials have also been evaluated, given below. These values are modest in comparison. As indicated in the main text, cost-supply curves were calculated for wave and tidal systems only. For presentation in this work only, these two cost-supply curves were combined into a single one for ocean energy. Parameters for regional ocean cost-supply curves are given in table S.4.3.

Wave Energy

In the case of wave energy, WEC (1994) estimated a maximum global installable capacity of 2 TW by limiting developments to technically favourable locations near coastlines. Using this value, and assuming a single capacity factor value of 32%, Krewitt et al. (2009) estimated a technical potential for wave energy of 20 EJ/yr, while UNDP (2000) estimated a technical potential of 65 EJ/yr using the same value but assuming a capacity factor of 100% instead. Following a more conservative approach restricted to shorelines exceeding a power production of 30 kW/m (resulting in around 2% of global coastlines), Sims et al. (2007) estimated a technical potential of 500 GW (6.3 EJ/y using a capacity factor of 40%). It is clear however that using single capacity factor values is not appropriate. It is likely that, as it is the case for wind, the cost variation of a wave energy cost-supply curve should stem from capacity factor variations which stem from the local quality of the resource. Such data is however not currently available as

it is for wind resources. Capacity factor distributions are likely to follow roughly those of wind energy, which vary between 15 and 35%, since both resources are closely related (wind capacity factor distributions were obtained by extracting the capacity factor from Hoogwijk et al. (2004) data). The assumption was therefore taken in this work that wave energy resources are captured using a single technology, with an investment cost given by ETSAP (2010a) of 6600 USD/kW, with a capacity factor that varies between 35% (where the resource quality is highest, and the cost of electricity production is lowest per unit energy produced) to a low value of 15% (below which sites are not economically useable). Using a maximum global capacity of 2 TW, the cost-supply curves were calculated with a hierarchical distribution, assuming that 90% of the wave resources are available at capacity factors within the range 15-35%. The disaggregation into 179 countries was performed according to the lengths of their respective coastlines, using data from CIA (2011).

Tidal Energy

Accounting for most of the global installed capacity of ocean energy systems, tidal energy is the only technology that has reached a commercial scale, with approximately 523 MW installed at the end of 2010 (IEA, 2010a). WEC (1994) made a rough estimation of the technical potential of tidal energy of about 2000 TWh/y (7.2 EJ/y), 10% considered economical (Rodier, 1992; WPC and WEC, 1986). In a more detailed study, Hammons (1993) presented a global but non-exhaustive list of potential tidal sites that could be considered for development, including projected installed capacities and approximate annual outputs. The total output from these sites would be of almost 400 TWh/y (1.4 EJ/y). Hammons (1993) furthermore extrapolated that the inclusion of additional sites around the world not studied specifically in his work would result in a global technical potential for tidal energy likely to range between 500 and 1000 TWh/yr (1.8 – 3.6 EJ/y). The cost-supply curve for tidal energy was calculated using the range of cost values given in ETSAP (2010a) of 5000 to 6500 USD/kW. Existing capacity was assumed to have been built at costs below that range, while the sites reviewed by Hammons (1993) (400 TWh/y) were assumed to be associated with costs within the range. Additional sites were assumed to have costs above the range.

Ocean Thermal and Salinity

The state of development of ocean thermal and salinity gradient energy technologies is currently experimental and therefore large uncertainties accompany calculations of associated energy potentials (Sims et al. (2007)). Upper limits in the form of theoretical potentials have been calculated. Nihous (2007) estimated a theoretical potential for ocean thermal energy of 2.7 TW (85 EJ/yr or 23 652 TWh/yr)), which corresponds to the maximum amount of energy resources that could be extracted without disrupting significantly the temperature of the upper layers of the ocean in an steady state regime, using a one-dimensional model of oceanic temperature gradients. Using a similar method, Charlier and Justus (1993) produced a more conservative estimation for the theoretical potential of 1000 GWe (32 EJ/yr), assuming a capacity factor of 100%. However, according to von Arx (1974), such a level of heat extraction would imply a decrease in the ocean surface layer temperature of approximately 1°C. In order to avoid such a decrease, Charlier and Justus (1993) recommends a reduced estimate based on 10 TW of usable heat replenishment rate, corresponding to 100 GWe (3.2 EJ/y).

In the case of Salinity Gradient, based on average discharge and low flow discharge values, Skramesto et al. (2009) estimated the theoretical potential in the range of 1600 - 1700 TWh/yr (5.8 - 6.1 EJ/yr). Using a global discharge rate of fresh water to seas of 44 500 km^3 per year, Krewitt et al. (2009) estimated a theoretical potential of 2000 TWh (7.2 EJ/yr), value very similar to the estimate of Skramesto et al. (2009).

S.3.7. Oil

Oil resources (Table S.4.6) were considered in four types of occurrences, crude oil, oil shales, extra-heavy oil and oil sands, following the data in BGR (2010) and WEC (2010). Cost information was obtained from IEA (2008). The data were aggregated into this work's world regions. For each type of occurrence for each region, a hierarchical distribution was parameterised by assuming that 1% of the resources have extraction cost below the lower bound, while 90% have a cost of extraction below the upper bound. The distributions were summed for each region in order to calculate regional cost-supply curves, and all distributions were summed in order to determine the global cost-supply curves given in figure 4 of the main text.

The curve for the lower boundary of the uncertainty range was defined by assuming that only crude oil, extra-heavy oil and oil sands reserves are available, and that the rest is either unusable or does not exist. The most probable cost-supply curve was calculated assuming that crude oil, oil sands and extra-heavy reserves and resources are available, as well as oil shale resources, but no additional amounts. The curve for the upper boundary of the uncertainty range assumes that all reserves, resources and additional amounts are available, and that an additional amount of oil shales is discovered, evaluated at 50% of the current resources. This was done in order to compensate for the absence of speculative resources and lack of detailed information available for oil shale resources, which are likely to become larger if additional exploration is carried out, and will occur if (but only if) interest in oil shales intensifies.[6]

S.3.8. Natural gas

Gas occurrences were considered in five forms, of which four unconventional: conventional gas (BGR, 2010), shale gas (EIA, 2011), tight gas (BGR, 2010; UNDP, 2000), coalbed methane (Boyer and Bai, 1998) and methane hydrates (Boswell and Collett, 2011). The associated cost ranges were obtained from ETSAP (2010b). Of the unconventional forms, only shale gas has seen exploitation larger than experimental. An additional source of methane exists, which is thought very large, aquifer gas (UNDP, 2000). However, its potential being very speculative, no reliable information over costs of extraction was found, and thus these were not considered in the present study. Similarly, methane hydrates provide a very large source of natural gas, however, these resources occurring under the sea, and the methods of extraction very experimental, the costs of exploitation are very large, and due to large amounts of shale gas available at lower costs, it is unclear whether the world will see wide-scale exploitation of methane hydrates. All resources were distributed into this work's world regions, except for the methane hydrates, for which it is not clear whether they are situated within territorial waters or not, and thus were assigned to an international category. Regional cost-supply curves were calculated with the same method as oil, and the global cost-supply curve is an aggregation of all regions.

The curve for the lower boundary of the uncertainty range includes conventional gas reserves only. The most probable cost-supply curve includes conventional, shale and tight gas reserves, along with half the conventional, shale and tight gas resources. It moreover includes half of the coalbed methane reserves. The curve for the upper boundary of the uncertainty range includes all reserves and resources, including methane hydrates.

S.3.9. Coal

Although coal is a very common commodity and well known resource, information over its natural occurrences is not very detailed. Coal information was available from two sources (BGR, 2010; WEC, 2010), and table S.4.8 was constructed using a mixture of both. Where information was inconsistent, the larger amounts were kept (such inconsistencies were not frequent nor very large). Since BGR (2010) does not report coal resources in the complete classification (proven, probable and possible reserves or resources) for all countries, some elements of the table are nil. This situation is likely to be due to the large amounts of coal available with conventional mining techniques, and therefore most of the resources are considered reserves, and occurrences with lower productivity or higher costs are not reported. Coal formations occur in different forms which have different calorific contents. For similar mining and transport costs, the costs of coal in terms of energy produced are higher for lower grade coals. Coal resources were divided into two categories, hard coal, including anthracite and bituminous coal which posseses higher calorific contents of between 16 500 and 35 000 kJ/t BGR (2010), and soft coal, including sub-bituminous coal and lignite, with calorific contents between about 11 000 and 16 500 kJ/t. Note that these classifications are not strictly well defined in geological terms, and that coal occurrences exist that have intermediate properties. This stems from different geophysical processes taking place during the slow formation of these hydrocarbons.

The curves for the lower boundary of the uncertainty ranges for soft and hard coal include proven reserves only. The most probable curves include proven and probable reserves, and half of the proven and probable resources. The curves for the upper boundary of the uncertainty ranges include all proven, probable and possible amounts for both reserves and resources.

[6]For instance, if strong decarbonisation policies are implemented globally, oil shales are not likely to be explored much further, since they currently involve large processing costs and only small scale exploitation.

S.3.10. Uranium

Information for uranium occurrences is available from a survey of the IAEA (2009), which compiles data provided by all member countries. They are highly detailed with four classifications and four cost ranges, as seen in table S.4.9. As the amounts in each row of the table are cumulative (i.e. the data in one cell is inclusive of the sum of the cells to the left), with the associated cost values they correspond to cumulative distributions. Assuming that they should follow hierarchical distributions, the associated cumulative distribution may be fitted using a non-linear least squares method. Although a fit of a function with three parameters over four data points is hardly a reliable method to determine a best fit with any level of certainty, it nevertheless produced the best curves that could be interpolated between points, as was determined by close inspection of each fit. Note that additional data points were be defined in order to constrain the fits better, such as additional values at higher costs by repeating the last data point, assumed equal to the technical potential in the saturation region, and at (0,0). The resulting fits were found to follow the data very closely. Values for military stocks of U are uncertain, since the information that is publicly available is scarce and incomplete, and were omitted. These are very small in comparison to natural stocks (IAEA, 2009).

The curve for the lower boundary of the uncertainty range includes only RAR (reasonably assured reserves) in all cost ranges. The most probable curve includes RAR and inferred reserves. The curve for the upper boundary of the uncertainty range includes all four classifications of resources in all cost ranges. The speculative resources in the unassigned cost range were not included in the non-linear fitting procedure, since their distribution into existing or higher cost ranges is ambiguous. They were therefore added to the technical potential of the upper boundary of the uncertainty range. Finally, it was assumed that sea water U is too costly and uncertain to include in the present study. Given the large amount of sea water on the planet, this resources is thought very large even though the concentration of U in sea water is very low. However, due to the very slow mixing process of sea water, it is misleading to consider the global body of sea water as a usable source of U, as it could be rapidly depleted locally, providing small amounts, without access to the remaining resources situated far offshore (Bonche, 2002).

S.3.11. Thorium

Thorium (Th) deposits in the Earth's crust around the world are expected to be three times larger than those of U, as determined from isotope lifetimes and the composition of the accreted material which formed the planet (Bonche, 2002; Sinha and Kakodkar, 2006; Abu-Khader, 2009; Suess and Urey, 1956)[7]. However, known resources of Th are much smaller and less detailed than those of U, a situation which is the result of the relatively small interest that has been given to Th in comparison to U. Therefore, it is to be expected that Th resources increase in size significantly if at some time in the future interest grows in Th based nuclear reactors. Although the Th nuclear fuel cycle has been demonstrated several decades ago, it has not been used commercially as it involves more safety hazards related to radiation than the U fuel cycle (Bonche, 2002; Sinha and Kakodkar, 2006). The Th nuclear fuel cycle is more efficient than that of U and therefore, involves less mass of Th per unit of electricity produced. For similar mining costs, Th resources are less expensive per unit of energy, however, the processing of Th into ^{233}U for fuel preparation has not been performed at an industrial scale. Therefore, the cost variable in the Th cost-supply curve is highly uncertain.

Data for Th resources were obtained from IAEA (2009). These are provided with much less detail than for U, with four uncertainty ranges but only one cost category. Consequently, the strategy of curve-fitting cannot be applied here, and one distribution of the non-interchangeable type per uncertainty category per world region was parametrised in the same way as for fossil resources. The cost axis was transformed from a cost per unit of mass to a cost per unit of energy using the efficiency of the Indian experimental model reported by Sinha and Kakodkar (2006) of 2100 TJ/t. The curve for the lower boundary of the uncertainty range includes RAR only. The most probable curve includes RAR and inferred reserves. The curve for the upper boundary of the uncertainty range includes all four categories.

References

3TIER, 2011a. Global solar irradiance map.
URL http://www.3tier.com

[7]Such arguments, which originates from astrophysics and the study of stars and nebulae, along with nuclear lifetimes of isotopes which were formed through nuclear reactions within stars or during supernova events, enable the prediction of relative amounts on Earth for all isotopes of elements of the periodic table (see for instance Suess and Urey (1956)).

3TIER, 2011b. Global wind speed map.
URL http://www.3tier.com
Abu-Khader, M. M., 2009. Recent advances in nuclear power: A review. PROGRESS IN NUCLEAR ENERGY 51 (2), 225–235.
Aldrich, M. J., Laughlin, A. W., Gambill, D. T., 1981. Geothermal resource base of the world: A revision of the electrical power research institute's estimate. Tech. rep., Los Alamos Scientific Laboratory, University of California.
Bertani, R., 2010. Geothermal power generation in the world. 2005-2010 update report.
Bertani, R., 2012. Geothermal power generation in the world 2005 - 2010 update report. Geothermics 41 (0), 1 – 29.
BGR, 2010. Reserves, Resources and Availability of Energy Resources. BGR.
Bonche, P., 2002. Le Nucleaire Explique par des Physiciens. EDP Sciences.
Boswell, R., Collett, T. S., 2011. Current perspectives on gas hydrate resources. Energy & Environmental Science 4 (4), 1206–1215.
Boyer, C. M., Bai, Q. Z., 1998. Methodology of coalbed methane resource assessment. International Journal of Coal Geology 35 (1-4), 349–368.
Cavanagh, J. E., Clarke, J. H., Price, T., 1993. Ocean Energy Systems. In: Johansson, T. B., Kelly, H., Reddy, A. K. N., Williams, R. H. (Eds.), Renewable Energy. Sources for Fuels and Electricity. Island Press.
Charlier, R. H., Justus, J. R., 1993. Ocean Energies: Environmental, Economic and Technological Aspects of Alternative Power Sources. Elsevier Oceanography Series.
CIA, 2011. The World Factbook. Central Intelligence Agency.
EIA, 2011. World Shale Gas Resources: An Initial Assessment of 14 Regions Outside the United States. EIA.
EPRI, 1978. Geothermal Energy Prospects for the Next 50 Years. EPRI.
ETSAP, I., 2010a. Marine energy. Tech. rep., IEA.
ETSAP, I., 2010b. Unconventional oil & gas production. Tech. rep., IEA ETSAP.
Hammons, T. J., 1993. Tidal Power. Proceedings of the IEEE 81 (3), 419–433.
Hoogwijk, M., 2004. On the global and regional potential of renewable energy sources. Ph.D. thesis, Universiteit Utrecht.
Hoogwijk, M., de Vries, B., Turkenburg, W., SEP 2004. Assessment of the global and regional geographical, technical and economic potential of onshore wind energy. Energy Economics 26 (5), 889–919.
Hoogwijk, M., Faaij, A., de Vries, B., Turkenburg, W., 2009. Exploration of regional and global cost-supply curves of biomass energy from short-rotation crops at abandoned cropland and rest land under four ipcc sres land-use scenarios. Biomass & Bioenergy 33 (1), 26–43.
Hoogwijk, M., Faaij, A., Eickhout, B., de Vries, B., Turkenburg, W., 2005. Potential of biomass energy out to 2100, for four ipccsres land-use scenarios. Biomass & Bioenergy 29 (4), 225–257.
IAEA, 2009. Uranium 2009: Resources, Production and Demand. IAEA/OECD/NEA.
IEA, 2008. World Energy Outlook 2008. IEA/OECD.
IEA, 2010a. Annual report 2010. implementing agreement on ocean energy systems. Tech. rep., IEA.
IEA, 2010b. Projected Costs of Generating Electricity 2010. IEA/OECD.
IEA, 2010c. Renewable energy essentials: Geothermal. Tech. rep., IEA.
IJHD, 2011. 2011 world atlas and industry guide. Tech. rep., The International Journal on Hydropower and Dams, Wallington, Surrey, UK.
IPCC, 2000. Emission Scenarios. Cambridge University Press.
Krewitt, W., Nienhaus, K., Klessmann, C., Capone, C., Stricker, E., Graus, W., Hoogwijk, M., Supersberger, N., von Winterfeld, U., Samadi, S., 2009. Role and potential of renewable energy and energy efficiency for global energy supply. Tech. rep., German Federal Environment Agency.
Lako, P., Eder, H., de Noord, M., Reisinger, H., 2003. Hydropower development with a focus on asia and western europe, overview in the framework of vleem 2. Tech. rep., ECN Policy Studies and Verbundplan.
Mork, G., Barstow, S., Kabuth, A., Pontes, M. T., 2010. Assessing the Global Wave Energy Potential. In: OMAE2010 - 29th International Conference on Ocean, Offshore Mechanics and Arctic Engineering.
Nihous, G. C., 2007. A preliminary assessment of ocean thermal energy conversion resources. Journal of Energy Resources Technology-Transactions of the ASME 129 (1), 10–17.
Pelc, R., Fujita, R., 2002. Renewable energy from the ocean. MARINE POLICY 26 (6), 471–479.
Rodier, M., 1992. Tidal Power: Trends and Developments. In: Proceedings of the 4th Conference on Tidal Power.
Rowley, J. C., 1982. Worldwide Geothermal Resources. In: Edwards, L. M., Chilingar, G. V., Rieke, H. H., Fertl, W. H. (Eds.), Handbook of Geothermal Energy. Houston, pp. 44–174.
Sims, R. E. H., Schock, R. N., Adegbululgbe, A., Fenhann, J., Konstantinaviciute, I., Moomaw, W., Nimir, H. B., Schlamadinger, B., Torres-Martinez, J., Turner, C., Uchiyama, Y., Vuori, S. J. V., Wamukonya, N., Zhang, X., 2007. Energy supply. In: Metz, B., Davidson, O., Bosch, P., Dave, T., Meyer, L. (Eds.), Climate Change 2007: Mitigation. Contribution of Working Group III to the Fourth Assessment Report of the Intergovernmental Panel on Climate Change. Cambridge University Press.
Sinha, R. K., Kakodkar, A., 2006. Design and development of the AHWR - the Indian thorium fuelled innovative nuclear reactor. Nuclear Engineering and Design 236 (7-8), 683–700.
Skramesto, O. S., Skilhagen, S. E., Nielsen, W. K., 2009. Power Production Based on osmotic Pressure. In: Waterpower XVI, Spokane, WA, USA.
Sørensen, B., 2011. Renewable energy : physics, engineering, environmental impacts, economics & planning. Academic Press.
Stefansson, V., 2005. World Geothermal Assessment. In: World Geothermal Congress, Antalya, Turkey.
Suess, H. E., Urey, H. C., Jan 1956. Abundances of the elements. Rev. Mod. Phys. 28, 53–74.
URL http://link.aps.org/doi/10.1103/RevModPhys.28.53
Tester, J. W., Anderson, B. J., 2006. Impact of enhanced geothermal systems (egs) on the united states in the 21st century. In: The Future of Geothermal Energy. Massachusetts Institute of Technology.
UNDP, 2000. World Energy Assessment. UNDP.
UNEP, 2011. Solar and wind energy resource assessment (swera): Renewable energy resource explorer (rrex).
URL http://swera.unep.net/
von Arx, W. S., 1974. Energy - Natural Limits and Abundances. Transactions-American Geophysical Union 55 (9), 828–832.
WEC, 1994. New Renewable Energy Resources: A Guide to the Future. WEC.

WEC, 2010. 2010 Survey of Energy Resources. WEC.
WPC, WEC, 1986. Survey of Energy Resources. Central Office, World Power Conference.

S.4. Data tables and figures

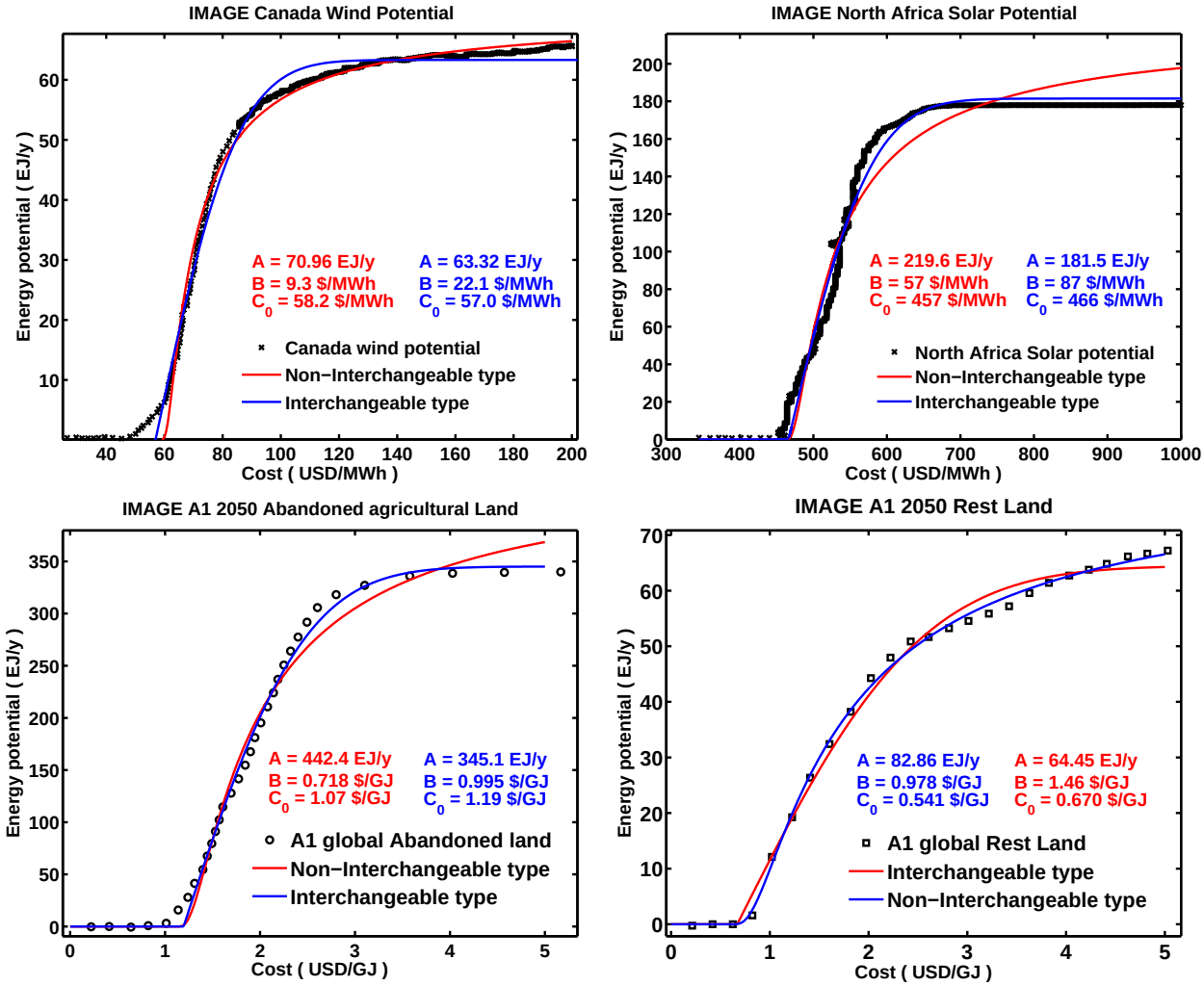

Figure S.4.1: Curve adjustments using non-linear least-squares of the two types of cumulative distribution with data from various studies of renewable energy potentials previously reported, calculated using the model IMAGE (reproduced from Hoogwijk et al. (2009, 2004); Hoogwijk (2004)). The goodness of these fits are a good indication for which type of distribution represents best each type of resource. It can observed that data for abandoned agricultural land is well described by the cumulative distribution for interchangeable resources (*top left*), while the data for rest land is described by the cumulative distribution of the non-interchangeable type (*top right*). Data for wind energy is well described as non-interchangeable resource units (*bottom left*), while the data for solar energy is well described as interchangeable resource units (*bottom right*).

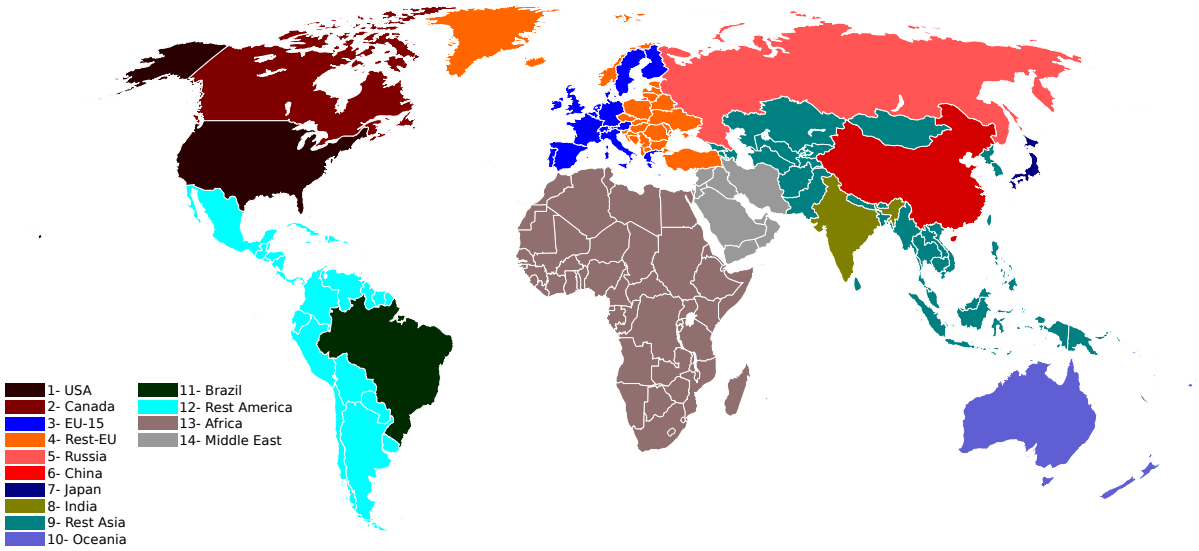

Region	Member countries
USA	USA
Canada	Canada
EU-15	Austria, Belgium, Danemark, Finland, France, Germany, Greece, Ireland, Italy, Luxemburg, Netherlands, Portugal, Spain, Sweden, United Kingdom
Rest Europe	Albania, Belarus, Bosnia-Herzegovina, Bulgaria, Croatia, Cyprus, Czech Rep., Estonia, Hungary, Iceland, Latvia, Lithuania, Macedonia, Malta, Moldova, Montenegro, Norway, Poland, Romania, Serbia, Slovakia, Slovenia, Switzerland, Turkey, Ukraine
Russia	Russia
China	China
Japan	Japan
India	India
Rest Asia	Afghanistan, Armenia, Azerbaijan, Bangladesh, Bhutan, Brunei, Cambodia, Georgia, Hong Kong, Indonesia, Kazakhtan, Korea, Kyrghizstan, Laos, Malaysia, Mongolia, Myanmar, Nepal, Pakistan, Philippines, Singapore, Taiwan, Tajikistan, Thailand, Turkmenistan, Uzbeksitan, Viet Nam
Oceania	Australia, New Zealand, Papua New Guinea, pacific islands
Brazil	Brazil
Rest America	Mexico, Central America, South America excluding Brazil
Africa	Africa
Middle East	Barhain, Iran, Iraq, Israel, Jordan, Kuwait, Lebanon, Oman, Palestine, Qatar, Saudi Arabia, Syria, UAE, Yemen

Table S.4.1: Definition of world regions for this paper with member countries for each.

Renewable cost-supply curve parameters									
	Hydro			Wind			Solar		
	Hierarchical			Hierarchical			Nearly identical		
Region	A	B	C_0	A	B	C_0	A	B	C_0
Name	PJ/y	\$/MWh	\$/MWh	PJ/y	\$/MWh	\$/MWh	PJ/y	\$/MWh	\$/MWh
USA	5 746	198.40	1.40	75 600	30.19	154.69	41 417	350.03	616.51
Canada	4 217	38.82	78.06	43 505	10.17	158.45	13 028	1542.58	835.33
EU-15	3 066	22.01	88.25	12 009	65.77	122.77	10 151	817.28	612.28
R. Eur.	4 283	54.13	38.85	32 183	19.38	151.30	9 815	679.12	716.41
Russia	6 595	82.84	75.89	38 774	65.10	138.90	55 081	428.97	607.22
China	11 502	26.37	35.65	6 057	175.01	170.21	110 427	241.71	691.85
Japan	846	25.24	82.31	360	109.24	170.21	2 456	185.69	836.16
India	2 788	103.23	0.00	2 018	109.62	217.65	43 846	140.01	479.40
R. Asia	7 227	160.05	0.00	18 125	83.64	132.94	75 845	348.99	486.13
Oceania	779	71.64	0.00	50 410	59.23	147.77	191 376	140.78	517.36
Brazil	4 738	18.45	12.00	13 248	23.33	136.55	40 604	310.45	523.59
R. Amer.	7 414	127.92	0.00	22 752	30.14	142.13	64 495	256.46	523.48
Africa	5 767	69.16	64.42	23 106	143.77	170.21	545 142	154.21	454.54
Mid. East	1 094	304.10	0.00	7 200	109.62	217.65	135 875	172.80	433.94
Total	66 061			345 348			1 339 560		

Table S.4.2: Table of cost-supply curve parameters for each region for hydro, wind and solar power.

Renewable cost-supply curve parameters						
	Wave			Tidal		
	Hierarchical			Hierarchical		
Region	A	B	C_0	A	B	C_0
Name	PJ/y	\$/MWh	\$/MWh	PJ/y	\$/MWh	\$/MWh
USA	496	36.68	227.64	145	89.18	303.33
Canada	5030	36.68	227.64	757	89.18	303.33
EU-15	1525	36.68	227.64	287	89.18	303.33
R. Eur.	2442	36.68	227.64	333	89.18	303.33
Russia	937	36.68	227.64	743	89.18	303.33
China	361	36.68	227.64	49	89.18	303.33
Japan	741	36.68	227.64	101	89.18	303.33
India	174	36.68	227.64	89	89.18	303.33
R. Asia	2843	36.68	227.64	396	89.18	303.33
Oceania	1536	36.68	227.64	238	89.18	303.33
Brazil	186	36.68	227.64	25	89.18	303.33
R. Amer.	1303	36.68	227.64	253	89.18	303.33
Africa	1027	36.68	227.64	140	89.18	303.33
Mid. East	309	36.68	227.64	42	89.18	303.33
Total	18 910			3600		

Table S.4.3: Table of cost-supply curve parameters for each region for wave and tidal energy.

Primary biomass cost-supply curve parameters								
	A1				A2			
Region Name	A EJ/y	B $/MWh	C_0 $/MWh	Type	A EJ/y	B $/MWh	C_0 $/MWh	Type
USA	51 082	3.93	7.68	2	34 082	6.42	7.23	2
Canada	20 000	1.64	7.68	2	15 000	1.50	7.73	2
EU-15	10 498	1.62	10.23	2	11 305	0.93	10.31	2
Rest Europe	11 660	0.41	10.38	2	10 784	1.45	7.57	2
Russia	124 033	1.73	7.68	2	70 451	1.96	7.29	2
China	102 113	11.26	9.12	1	24 320	9.92	11.33	2
Japan	32	0.69	11.28	2	12	9.98	18.53	2
India	24 023	3.37	7.08	2	13 756	2.32	6.99	2
Rest Asia	11 812	0.93	7.56	2	8 627	0.35	7.65	2
Oceania	53 576	2.01	7.22	2	34 477	3.31	6.65	2
Brazil	76 867	1.33	10.62	2	23 838	5.12	7.94	2
Rest America	27 513	2.06	9.52	2	8 542	3.49	7.57	2
Africa	134 245	4.32	5.76	2	51 240	6.70	3.27	2
Middle East	13 011	25.38	11.04	1	8 011	13.08	11.33	2
Total	660 438				314 438			
	B1				B2			
Region Name	A EJ/y	B $/MWh	C_0 $/MWh	Type	A EJ/y	B $/MWh	C_0 $/MWh	Type
USA	36 082	0.85	7.70	2	50 082	2.07	6.41	2
Canada	16 000	0.84	6.30	2	16 000	0.94	6.41	2
EU-15	8 075	3.29	8.63	1	12 921	4.77	7.30	1
Rest Europe	10 039	2.49	6.29	1	12 181	0.45	8.52	2
Russia	89 304	0.99	6.30	2	79 381	0.94	6.41	2
China	79 174	1.57	6.30	2	47 259	5.51	10.01	2
Japan	32	0.69	9.90	2	62	0.69	10.01	2
India	13 756	3.35	5.62	2	5 356	5.24	6.41	2
Rest Asia	5 093	0.72	6.19	2	4 348	1.85	6.60	2
Oceania	35 279	0.96	5.51	2	29 279	0.87	5.90	2
Brazil	56 539	4.76	7.14	1	39 747	2.29	8.84	2
Rest America	19 841	3.88	5.70	2	10 634	12.26	6.41	1
Africa	81 240	3.39	5.20	2	15 236	4.87	3.74	2
Middle East	4 011	4.99	9.90	2	3 011	5.49	10.01	2
Total	454 438				325 438			

Table S.4.4: Table of cost-supply curve parameters for biomass primary energy resources for four SRES scenarios A1, A2, B1 and B2.

Geothermal energy cost-supply curve parameters												
	Direct Use						Electricity					
	In belt			Out of belt			In belt			Out of belt		
	Hierarchical			Nearly identical			Hierarchical			Nearly identical		
Region	A	B	C_0	A	B	C_0	A	B	C_0	A	B	C_0
Name	PJ/y	$/MWh	$/MWh	PJ/y	$/MWh	$/MWh	PJ/y	$/MWh	$/MWh	PJ/y	$/MWh	$/MWh
USA	70	7.22	94.34	130	81.44	118.44	1290	20.62	144.96	2395	63.62	255.71
Canada	9	7.22	94.34	78	81.44	118.44	240	20.62	144.96	2160	63.62	255.71
EU-15	1	7.22	94.34	84	81.44	118.44	13	20.62	144.96	1381	63.62	255.71
R. Eur.	12	7.22	94.34	26	81.44	118.44	116	20.62	144.96	496	63.62	255.71
Russia	9	7.22	94.34	168	81.44	118.44	261	20.62	144.96	4951	63.62	255.71
China	42	7.22	94.34	98	81.44	118.44	766	20.62	144.96	1788	63.62	255.71
Japan	14	7.22	94.34	0	81.44	118.44	136	20.62	144.96	0	63.62	255.71
India	2	7.22	94.34	35	81.44	118.44	37	20.62	144.96	704	63.62	255.71
R. Asia	109	7.22	94.34	86	81.44	118.44	1419	20.62	144.96	1404	63.62	255.71
Oceania	19	7.22	94.34	76	81.44	118.44	210	20.62	144.96	1561	63.62	255.71
Brazil	5	7.22	94.34	91	81.44	118.44	97	20.62	144.96	1840	63.62	255.71
R. Amer.	135	7.22	94.34	86	81.44	118.44	1923	20.62	144.96	1470	63.62	255.71
Africa	51	7.22	94.34	199	81.44	118.44	721	20.62	144.96	3959	63.62	255.71
Mid East.	10	7.22	94.34	47	81.44	118.44	178	20.62	144.96	853	63.62	255.71
Total	487			1 203			7 407			24 962		

Table S.4.5: Table of cost-supply parameters for geothermal energy, for both direct use of heat and electricity production.

Oil	Mtoe								
	Crude Oil		Oil Shales	Oil Sands			Extra Heavy Oil		
Region	BGR (2010)		WEC (2010)	WEC (2010)			WEC (2010)		
Name	Reserves	Resources	Resources	Reserves	Resources	Additional	Reserves	Resources	Additional
USA	3 863	10 000	536 931	0	5 429	2 388	3	379	4
Canada	667	2 400	2 192	24 909	227 189	355 828	0	0	0
EU-15	1 193	1 545	13 248	31	276	0	24	1 928	0
Rest Europe	1 155	3 530	4 411	0	1	0	5	51	0
Russia	10 436	16 400	35 470	4 147	39 034	7 505	1	25	0
China	2 018	2 300	47 600	0	233	0	110	1 168	0
Japan	6	10	0	0	0	0	0	0	0
India	792	400	0	0	0	0	0	0	0
Rest Asia	9 218	10 535	3 988	6 203	55 945	0	18	1 163	0
Oceania	595	1 100	4 534	0	0	0	0	0	0
Brazil	2 450	5 000	11 734	0	0	0	0	0	0
Rest America	8 996	9 588	60	0	136	0	8 476	270 637	27 704
Africa	17 277	15 485	23 317	263	2 364	6 778	7	66	0
Middle East	102 366	21 170	5 792	0	0	0	0	0	0
Total	161 031	99 463	689 277	35 552	330 607	372 500	8 644	275 416	27 707

Costs	USD2008 / boe	IEA (2008)							
	Crude Oil		Oil Shales	Oil Sands			Extra Heavy Oil		
	Reserves	Resources	Resources	Reserves	Resources	Additional	Reserves	Resources	Additional
Upper	10	10	50	40	40	40	10	40	10
Lower	40	100	100	50	70	70	50	70	70

Table S.4.6: Oil resources by world region in units of Mtoe (million tonnes of oil).

Gas	$10^9 m^3$									
	Conv. gas		Shale gas		Tight gas		Coalbed Methane		Methane Hydrates	
Region	BGR (2010)		EIA (2011)		BGR (2010)		Boyer and Bai (1998)		Boswell (2011)	
Name	Reserves	Resources	Reserves	Resources	Reserves	Resources	Reserves	Resources	Reserves	Resources
USA	7 080	20 000	17 000	45 600	1000	210 000	9 700	2 000	0	0
Canada	1 754	7 000	10 988	42 198	0	7 000	5 700	70 800	0	0
EU-15	2 338	2 530	7 024	28 547	0	7 000	2 802	0	0	0
R. Eur.	3 889	7 510	9 374	39 734	0	0	1 908	0	0	0
Russia	47 578	105 000	538	2 152	0	45 000	17 000	96 300	0	0
China	2 455	10 000	36 109	144 463	0	9 000	30 000	5 100	0	0
Japan	21	5	0	0	0	0	0	0	0	0
India	1 115	900	1 784	8 213	0	1 000	800	0	0	0
Rest Asia	23 951	22 805	1 444	5 834	0	0	1 100	0	0	0
Oceania	3 553	2 450	11 215	39 111	0	1 000	8 500	5 700	0	0
Brazil	365	2 000	7 533	25 658	0	6 000	0	0	0	0
R. Amer.	7 704	8 858	47 579	170 745	0	0	0	0	0	0
Africa	14 753	16 155	29 482	112 206	0	0	800	0	0	0
Mid. East	75 358	35 370	0	0	0	0	0	0	0	0
International	0	0	0	0	0	38 000	0	0	300 000	300 000
Total	191 914	240 583	180 070	1 0748 62	1 000	324 000	78 310	179 900	300 000	300 000

Costs	USD2008 / GJ		ETSAP (2010b)							
	Conv. gas		Shale gas		Tight gas		Coalbed Methane		Methane Hydrates	
	Reserves	Resources	Reserves	Resources	Reserves	Resources	Reserves	Resources	Reserves	Resources
Upper	0.5	0.5	3.8	3.8	2.6	2.6	3.8	3.8	4.4	4.4
Lower	5.7	5.7	8.6	8.6	7.6	7.6	7.6	7.6	8.6	8.6

Table S.4.7: Natural gas resources by world region in units of Gm^3 (billion cube meters).

Coal	Mt					
	Hard coal					
	Reserves			Resources		
Region Name	Proven WEC (2010)	Probable BGR (2010)	Possible	Proven WEC (2010)	Probable BGR (2010)	Possible
USA	226 694	0	0	6 691 942	0	0
Canada	4 346	0	0	187 606	0	0
EU-15	84 721	0	0	278 420	0	0
Rest Europe	24 534	752	1 862	254 658	7 428	11 422
Russia	68 655	0	0	2 730 810	0	0
China	180 600	0	0	681 600	0	0
Japan	340	0	0	4 603	1 988	7 375
India	56 100	0	0	105 820	123 470	37 920
Rest Asia	54 678	0	0	289 048	0	0
Oceania	44 627	0	0	1 620 675	0	0
Brazil	1 547	0	0	6 212	0	0
Rest America	9 960	4572	4 237	20 496	0	0
Africa	32 546	0	0	58 150	0	0
Middle East	1 203	0	0	41 203	0	0
Total	790 551	5 324	6 099	12 971 243	132 886	56 717
	Soft coal					
	Reserves			Resources		
Region Name	Proven WEC (2010)	Probable BGR (2010)	Possible	Proven WEC (2010)	Probable BGR (2010)	Possible
USA	30 851	0	0	1 398 669	0	0
Canada	3 108	0	0	17 371	40 055	108 995
EU-15	44 214	0	0	89 158	0	0
Rest Europe	40 456	1 996	3 124	275 185	14 961	11 581
Russia	91 350	0	0	1 371 030	0	0
China	52 300	0	0	318 000	0	0
Japan	10	0	0	160	1 132	4 074
India	4 895	0	0	38 647	0	0
Rest Asia	30 762	7 086	34 070	387 263	11 871	57 198
Oceania	37 738	62 840	101 100	46 973	73 102	112 300
Brazil	4 559	7 559	4 575	6 513	10 799	6 535
Rest America	5 633	527	790	7 524	0	0
Africa	180	0	0	338	0	0
Middle East	0	0	0	0	0	0
Total	346 056	80 008	143 659	3 956 831	151 920	300 683

Costs	USD2008 / t	IEA (2008)				
	Reserves			Resources		
	Proven	Probable	Possible	Proven	Probable	Possible
	20	20	20	20	20	20
	50	50	50	100	100	100

Table S.4.8: Coal resources by world region in units of Mt (million tonnes of coal). Hard coal includes anthracite and bituminous coal, while soft coal includes sub-bituminous coal and lignite. Since there is no clear demarcation between ranks of coal, the limit is put onto the calorific content, and thus coal resources with a calorific content higher than 16 500 kj/t belong to the hard coal category (as defined in BGR (2010)), while coal resources with a lower calorific content belong to soft coal. Anthracite can have calorific contents of up to 35 000 kJ/t while lignite can have calorific values as low as 11 000 kJ/t.

Uranium	t	IAEA (2009)						
Region	Reasonably Assured Reserves (RAR)				Inferred			
Name	<40$/kg	<80$/kg	<130$/kg	<260$/kg	<40$/kg	<80$/kg	<130$/kg	<260$/kg
USA	0	39 000	207 400	472 100	0	19 500	103 700	236 050
Canada	267 100	336 800	361 100	387 400	99 700	110 600	124 200	157 200
EU-15	0	7 000	20 800	33 800	0	0	13 500	110 400
Rest Europe	2 500	39 100	88 500	160 000	3 200	15 000	43 850	109 850
Russia	0	100 400	181 400	181 400	0	57 700	298 900	384 900
China	52 000	100 900	115 900	115 900	15 400	49 100	55 500	55 500
Japan	0	0	6 600	6 600	0	0	3 300	3 300
India	0	0	55 200	55 200	0	0	23 900	24 900
Rest Asia	14 600	326 600	454 500	533 500	29 800	276 800	366 000	474 900
Oceania	0	1 163 000	1 176 000	1 179 000	0	449 000	497 000	500 000
Brazil	139 900	157 700	157 700	157 700	0	73 600	121 000	121 000
Rest America	0	7 000	11 700	13 800	0	4 400	10 100	11 300
Africa	93 800	194 600	644 100	663 400	78 500	121 800	260 000	286 300
Middle East	0	44 000	44 000	44 700	0	67 800	67 800	69 200
Total	569 900	2 516 100	3 524 900	4 004 500	226 600	1 245 300	1 989 750	2 544 800
Region	Prognosticated				Speculative			
Name		<80$/kg	<130$/kg	<260$/kg		<130$/kg	<260$/kg	Unassigned
USA		819 500	1 169 300	1 036 950		858 000	858 000	482 000
Canada		50 000	150 000	150 000		700 000	700 000	0
EU-15		7 000	7 600	7 600		50 100	50 100	94 000
Rest Europe		200	41 650	66 650		6 650	126 650	314 000
Russia		0	182 000	182 000		0	0	633 000
China		3600	3 600	3 600		4 100	4 100	0
Japan		0	3 300	3 300		3 300	3 300	0
India		0	0	63 600		0	0	17 000
Rest Asia		377 900	591 400	592 900		1 776 600	1 806 100	264 700
Oceanial		300 000	300 000	300 000		0	0	500 000
Brazil		73 600	121 000	121 000		121 000	121 000	0
Rest America		6 600	23 500	23 500		236 700	236 700	176 200
Africa		49 400	156 900	156 900		25 000	25 500	1 112 900
Middle East		67 800	89 000	89 000		84 800	98 800	0
Total		1 755 600	2 839 250	2 797 000		3 866 250	4 029 750	3 593 800

Table S.4.9: Uranium resources (in natural concentration) by world region in units of tonnes.

Thorium	t	IAEA (2009)		
Region	RAR	Inferred	Indentified	Prognosticated
Name	< 80 USD/kg	< 80 USD/kg	< 80 USD/kg	N/A
USA	122 000	278 000	400 000	274 000
Canada	0	44 000	44 000	128 000
EU-15	0	0	0	0
Rest Europe	54 000	213 000	186 000	164 000
Russia	75 000	112 500	75 000	0
China	0	0	0	0
Japan	0	0	0	0
India	319 000	478 500	319 000	0
Rest Asia	0	0	0	0
Oceanial	46 000	406 000	452 000	0
Brazil	172 000	130 000	302 000	330 000
Rest America	0	300 000	300 000	0
Africa	18 000	127 000	118 000	410 000
Middle East	0	0	0	0
Unassigned	23 000	10 000	33 000	81 000
Total	829 000	2 099 000	2 229 000	1 387 000

Costs	USD2008 / kg			
	RAR	Inferred	Indentified	Prognosticated
Lower	40	40	40	80
Upper	80	80	80	260

Table S.4.10: Thorium resources (in natural concentration) by world region in units of tonnes.